Green Chemistry

ROYAL SOCIETY OF CHEMISTRY

CRITICAL REVIEW

View Article Online
View Journal | View Issue

Cite this: *Green Chem.*, 2025, **27**, 275

Advances of the past 12 years in decarboxylation of biomass carboxylic acids to biofuels and high-value chemicals *via* photo- or electrocatalysis

Chen-Qiang Deng and Jin Deng *

The utilization of renewable platform molecules as feedstocks for manufacturing high-value-added fine chemicals and liquid fuels has become crucial for green and sustainable chemistry and represents a rewarding challenge for today's society. Photochemistry and electrochemistry are effective and powerful tools for the transformation of biomass molecules through free radical intermediates under mild reaction conditions. Numerous direct decarboxylative reactions, without the need for prefunctionalization of carboxylic acids, by photocatalysis or electrocatalysis have been developed during the last few years, with more efficient, step-economical, and low energy consumption processes. In this review, we summarize recent advances in photochemical and electrochemical decarboxylative reactions for the synthesis of alkane fuels and high-value chemicals by utilizing biomass-derived free carboxylic acids as a sustainable source. These transformations can be categorized into four main types as follows: (1) decarboxylative reduction, (2) decarboxylative elimination, (3) decarboxylative coupling, and (4) decarboxylative oxidation. The scope and limitations of these conversions and mechanisms are discussed in detail. Finally, the challenges and perspectives for light or electrically driven decarboxylative transformation of renewable carboxylic acid feedstocks are proposed.

Received 24th September 2024,
Accepted 23rd November 2024

DOI: 10.1039/d4gc04788e

rsc.li/greenchem

1. Introduction

In the past few decades, environmental pollution problems and energy crises caused by the excessive consumption of fossil resources have aroused widespread concern in the scientific community. Due to the non-renewable nature of fossil resources, the exploration of green and sustainable routes has

Key Laboratory of Precision and Intelligent Chemistry, CAS Key Laboratory of Urban Pollutant Conversion, Anhui Province Key Laboratory of Biomass Chemistry, Department of Applied Chemistry, University of Science and Technology of China, Hefei, Anhui 230026, China. E-mail: dengjin@ustc.edu.cn

Chen-Qiang Deng

Chen-Qiang Deng is currently pursuing his Ph.D. in the Department of Applied Chemistry at the University of Science and Technology of China. His research focuses on converting biomass carboxylic acids into renewable fuels and high value-added chemicals through catalytic hydrogenation and photocatalysis technologies.

Jin Deng

Dr Jin Deng is an Associate Research Professor of Applied Chemistry at the University of Science and Technology of China. He specializes in developing and scaling up innovative, efficient, and stable catalytic methods to convert biomass and plastic waste into fuels and high-value chemicals. Additionally, he evaluates the carbon footprint of these green processes through life cycle assessment. His interdisciplinary research combines organic chemistry, chemical engineering, materials science, and environmental science to advance sustainable solutions.

become an ongoing endeavor for chemists. Lignocellulosic biomass is a non-edible and renewable starting material with an estimated amount of about 180 billion tonnes produced annually,[1] which mainly consists of cellulose (40–60%), hemicellulose (20–40%) and lignin (10–25 wt%), along with other minor components such as minerals, pectins, and extractives.[2] Lignocellulose, as the only renewable and sustainable organic carbon resource in nature, is an ideal alternative to fossil resources and can be used to manufacture bio-based chemicals and fuels.[3–8] Numerous studies have been devoted to the direct conversion of lignocellulosic biomass through chemical and biological catalysis.[9–12] However, the recalcitrance and structure complexity of lignocellulose bring huge challenges over its efficient utilization. An important transformation route is first to obtain carbohydrate substances from various biomass raw materials through enzymes or acids, and then further conversion into biomass-derived platform compounds such as levulinic acid,[13,14] furfural,[15] and lactic acids.[16,17] Utilizing furfural as a pivotal platform compound, a broad range of biomass-based molecules, such as tetrahydrofuroic acid,[18] 5-hydroxyvaleric acid,[19] and succinic acid,[20] have been manufactured through state-of-the-art technologies. Additionally, medium-long chain fatty acids and α,ω-dicarboxylic acids can be obtained by aldol condensation of biomass platform molecules such as furfural and levulinic acid, followed by the hydrodeoxygenation reaction.[21] In addition to biomass resources, lipid-rich wastes are an important renewable resource with low-value by-products produced in fat and oil processing and the pulp industry.[22,23] Bio-based long-chain fatty acids can be generated by saponification reactions from triglycerides, accompanied by the formation of glycerol. Moreover, many catalytic systems have been developed for the selective conversion of bio-based glycerol to obtain functionalized carboxylic acids, including glyceric acid,[24] lactic acids,[25] and alanine.[26,27]

As summarized in Fig. 1, biomass and lipids can supply a wide variety of alkyl carboxylic acids by state-of-the-art technologies, and their further conversion into useful molecules is essential. Utilizing bio-based aliphatic carboxylic acids as the starting material to undergo decarboxylative transformation has attracted considerable attention from chemists over the past few decades. Traditional thermal catalytic systems for C(sp^3)–COOH bond scission often require harsh conditions, typically involving high temperatures that are achieved through an energy-intensive process, leading to unwanted cracking and coke deposition.[28–30] Due to the direct decarboxylative inertness of aliphatic carboxylic acids, a detour approach is pre-activation, for instance, to form their redox-active esters.[31] However, this approach involves the downsides of requiring an additional synthetic step, fabrication of excessive waste, and diminished atom economy. Therefore, the pursuit of a direct decarboxylative process under milder conditions has become the key to the transformation of bio-based carboxylic acids into high-value chemicals and biofuels. In the past decade, photochemistry and electrochemistry have attracted extensive attention as efficient and powerful tools for sustainable chemical production from renewable biomass feedstocks.[32–38] Visible light has been recognized as a cost-effective and environmentally benign source of energy that promotes chemoselective molecular substrate activation, opening up broad horizons for the design and discovery of novel chemical transformations.[39] Photocatalytic decarboxylation is emerging as an effective approach that can make new carbon–carbon and carbon–heteroatom bonds in molecular substrates through radical chemistry processes under mild reaction conditions. In the past decades, considerable efforts have been devoted toward visible light-mediated direct decarboxylation of biomass-derived aliphatic carboxylic acids without additional pre-activation to generate carbon-centered radicals for achieving valuable transformation. Based on these important published works, we summarized that the general mechanism of photocatalytic radical decarboxylation can be roughly divided into the following four modes, as shown in Scheme 1. In the first mode, carboxylates (the conjugate bases

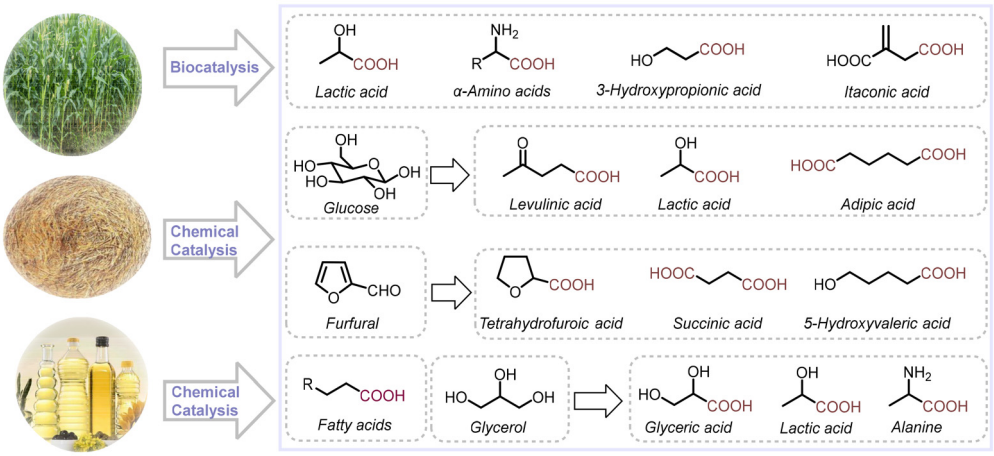

Fig. 1 Representative bio-based alkyl carboxylic acids in this review.

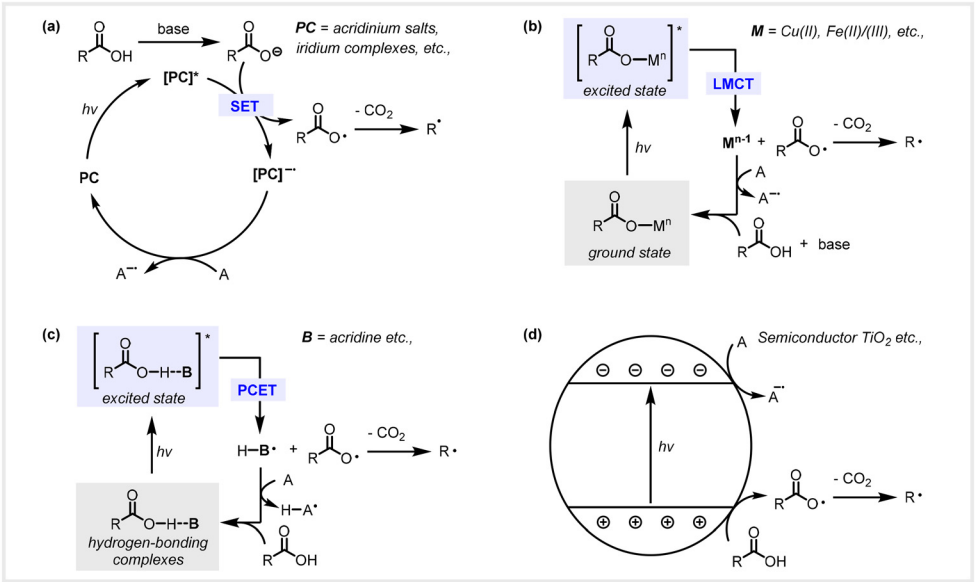

Scheme 1 General mechanism of the photocatalytic decarboxylative reaction. A, electron acceptor. SET, single electron transfer. LMCT, ligand–metal charge transfer. PCET, proton-coupled electron transfer.

of carboxylic acids) are oxidized by the excited state photocatalyst to generate carboxyl radicals through a single electron transfer (SET) event, which spontaneously extrude carbon dioxide and concomitantly generate carbon-centered radicals (Scheme 1a). Due to the high oxidation potential of the carboxylate, especially the non-α-heteroatom or benzyl-substituted aliphatic carboxylic acids, such photocatalysts (*e.g.*, organic acridinium and noble iridium-based complexes) with strong oxidation ability are often required.[40–42] In addition, adding a base is necessary for the deprotonation of carboxylic acids in this reaction. Another mode is the ligand exchange between carboxylic acids and metal salts for the generation of the ground-state carboxylate species, which is then excited upon light irradiation and undergoes homolysis through a ligand–metal charge transfer (LMCT) event to generate a carboxyl radical and low-valent metal center (Scheme 1b). In this type of transformation, such metal salt catalysts are typically a first transition metal center such as iron(III),[43] copper(II)[44] or the like. In the third mode, the hydrogen bonding complexes are formed between the carboxylic acid and the photocatalyst (*e.g.*, acridine), which generate the photoexcited states under visible light irradiation and undergo homolysis *via* a proton-coupled electron transfer (PCET) event to afford a carboxyl radical (Scheme 1c).[45–47] The advantage of this system can circumvent the high oxidation potential of free alkyl carboxylic acids and the use of bases in the reaction. Compared with the above three catalytic modes, semiconductor heterogeneous photocatalysis is completely different in the reaction mechanism. In heterogeneous photocatalysts such as TiO_2, when photons with energy higher than the semiconductor's band gap are absorbed, an electron is excited to the conduction band, simultaneously creating a hole in the valence band. The generated holes at the valence band have a strong oxidation ability that oxidizes the carboxylates, giving carboxyl radicals, which spontaneously extrude CO_2 and concomitantly generate carbon-centered radicals (Scheme 1d).[41]

Electrochemistry is regarded as an environmentally friendly and efficient synthesis tool with many unique advantages. The anode and cathode can continuously offer clean electrons as green redox agents, which avoids over-reliance or the use of dangerous or toxic oxidants and reducing agents, minimizing the production of reagent waste.[48] In addition, electrochemical reactions are simple to operate, generally carried out at room temperature and under atmospheric pressure, and can selectively oxidize functional groups.[49] Hence, the utilization of electrochemical strategies for the conversion of biomass-derived carboxylic acids to valuable chemicals holds great promise. In 1848, Kolbe discovered electrolysis of carboxylic acids in aqueous solution to afford symmetrical alkanes.[50] This classic electrochemical process involved the dimerization of free radical intermediates for the construction of C–C bonds. However, in some cases, the free radicals formed on the anode surface could be further oxidized into carbocations to generate by-products such as alkenes, inhibiting the Kolbe electrolysis reaction. The general mechanism for the anodic oxidative decarboxylation of alkyl carboxylic acids can be categorized into two types: (a) in the presence of a platinum electrode and high current density, the carboxylate lost one electron at the anode to generate free radical intermediates that dimerize to make C–C bonds, known as the Kolbe coupling reaction, and (b) the carboxylate lost two electrons at the anode to form carbocation intermediates which were subsequently captured using nucleophiles to provide the functionalized product, known as the Hofer–Moest reaction (Scheme 2).

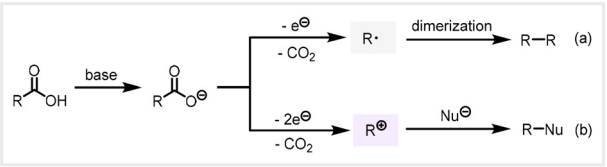

Scheme 2 General mechanism of electrochemical decarboxylation.

Despite numerous reviews on decarboxylative transformations found in the published studies,[51–54] this review mainly focuses on bio-based free alkyl carboxylic acids as feedstocks for sustainable conversion into high-value fine chemicals and liquid fuels through photocatalytic and electrocatalytic direct decarboxylation. With our continued interest in the green and efficient conversion of biomass alkyl carboxylic acids, our intention is to classify different reaction types and summarize the recent progress in various electrochemical and photochemical decarboxylative reactions based on utilizing bio-derived carboxylic acids as a sustainable source.

2. Photochemical decarboxylative reduction

2.1 Synthesis of biofuels

Decarboxylative reduction driven by light is an attractive strategy for the synthesis of liquid hydrocarbon fuels from renewable fatty acids because it can avoid the harsh reaction conditions of thermal catalysis such as high temperature and pressure. In 2015, the Nicewicz group developed a Fukuzumi-derived acridinium photoredox catalyst in combination with a phenyldisulfide to achieve the decarboxylative reduction of aliphatic carboxylic acids.[40] Trifluoroethanol (TFE) as the solvent was found to be essential for the decarboxylation. Under the optimized reaction conditions, long-chain tridecanoic acid was decarboxylated to afford dodecane using a TFE/EtOAc mixed solvent, with a moderate yield of 49%. Based on mechanistic experiments, the authors proposed a catalytic cycle for the photoredox decarboxylation (Scheme 3A). First, alkyl carboxylic acids were deprotonated by bases to form carboxylates. They then underwent single electron oxidation by the photoexcited Mes-Acr-Ph* to generate carboxyl radicals with subsequent extrusion of CO_2 furnishing the alkyl radical **G**. Hydrogen atom abstraction from thiophenol **D** *via* the alkyl radical afforded the corresponding products. Finally, the thiyl radical **E** reoxidized the species **C** to regenerate the photocatalyst and thiophenol, completing the catalytic cycle. In 2022, the Li group adopted a similar catalytic system to further expand the scope of fatty acids (Scheme 3B).[41] In the presence of a modified acridinium Mes-1,3,6,8-tetramethoxy-Acr-3″,5″-dimethoxy-Ph (PC) as the photocatalyst and *p*-tolyl disulfide as the hydrogen transfer catalyst, a series of fatty acids could be smoothly converted to C_{n-1} alkanes in high yields. This protocol utilized the inexpensive and green ethyl acetate/H_2O as the solvent.

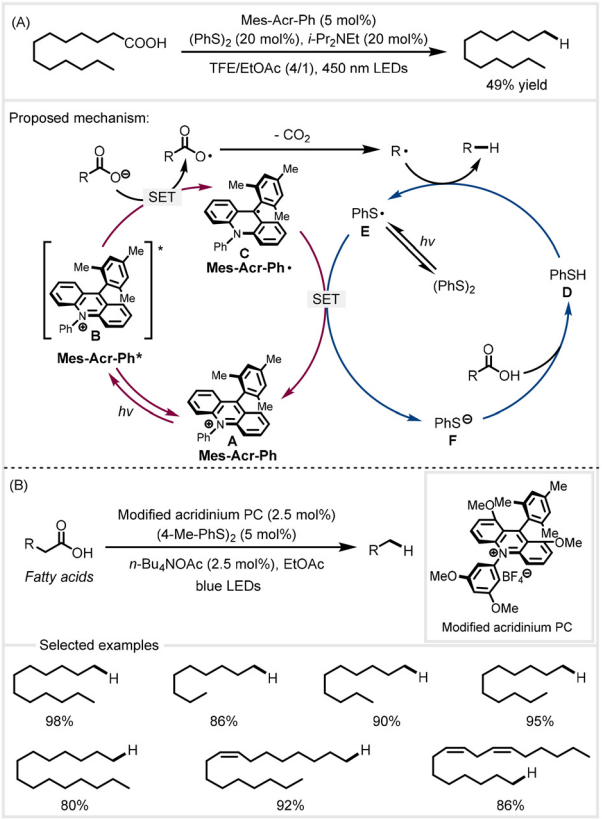

Scheme 3 Photoredox catalyzed decarboxylative reduction.[40,41]

The addition of *n*-Bu_4NOAc was essential for this decarboxylative reduction to occur.

In 2022, the Pospech group utilized pyrimidopteridine (PrPPT) as the photoredox catalyst to accomplish decarboxylative reduction of aliphatic carboxylic acids under visible light irradiation.[55] This reaction did not require external thiols as the hydrogen transfer catalyst. Regrettably, this protocol was relatively inefficient for the decarboxylative reduction of long-chain fatty acids, affording only 15–20% yields of alkane products. Mechanistic studies revealed that pyrimidopteridine plays the dual roles of a photoredox catalyst and a hydrogen atom transfer catalyst in this reaction. A catalytic cycle was proposed, as shown in Scheme 4. The deprotonation of carboxylic acids with K_3PO_4 formed aliphatic carboxylates, which then were oxidatively decarboxylated by photoexcited PrPPT* to generate the alkyl radical and radical anionic catalyst $PrPPT^{\bullet-}$. Next, $PrPPT^{\bullet-}$ was protonated by another molecule of carboxylic acid to give the $PrPPTH^{\bullet}$ species. Finally, the hydrogen atom transfer (HAT) process from $PrPPTH^{\bullet}$ to the alkyl radical afforded alkane products and regenerated the photocatalyst. Later, a base-free procedure was reported by Cavalcanti *et al.* to achieve the decarboxylative reduction of long-chain fatty acids with 9-(2-chlorophenyl)acridine as the photocatalyst and thiophenol as the co-catalyst.[47] Using dichloromethane as the solvent, a range of C_{n-1} alkanes could be obtained in high yields with excellent selectivity under 400 nm light irradiation.

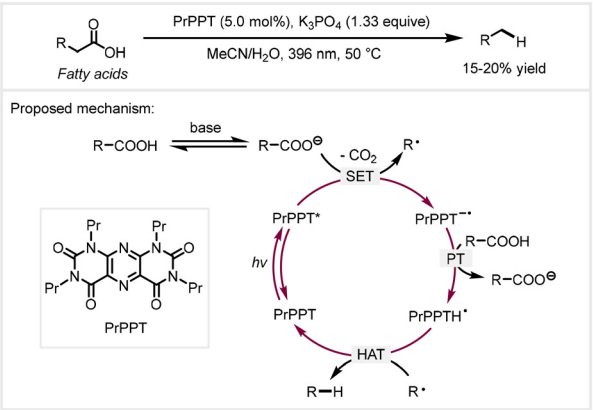

Scheme 4 Proposed mechanism of photocatalytic decarboxylative reduction.[55] PT: proton transfer. HAT: hydrogen atom transfer.

It is worth mentioning that licuri oil could be also transformed into a mixture of C_9–C_{17} hydrocarbons *via* a two-step procedure involving hydrolysis and decarboxylation.

In 2022, the West group developed a cooperative iron/thiol catalyst system to achieve the decarboxylative reduction of free alkyl carboxylic acids upon irradiation with visible light.[43] Under the optimized conditions, tridecanoic acid and oleic acid could be efficiently decarboxylated with a yield of 99%. Moreover, various complex molecules bearing carboxylic acid moieties were also tolerated. This protocol features good functional group tolerance and mild reaction conditions. Moreover, this decarboxylative reaction would also proceed in the absence of di(2-picolyl)amine as the ligand, but a slightly reduced yield was observed. According to mechanistic experiments and previous reports, the authors proposed a dual catalytic cycle (Scheme 5). The reaction of alkyl carboxylic acids with iron(III) salts formed iron(III) carboxylates **A**. They generated photoexcited iron(III) carboxylate **B** upon irradiation with visible light, which was then homolyzed to afford Fe(II) species **C** and carboxyl radicals **D** *via* a ligand–metal charge transfer (LMCT) process. Next, the carboxyl radical quickly extruded carbon dioxide to generate alkyl radical **E**. Hydrogen atom abstraction from thiol **G** *via* the alkyl radical afforded the corresponding products. Finally, the thiyl radical **F** reoxidized Fe(II) species and combined with another molecule of the acid to close the cycle.

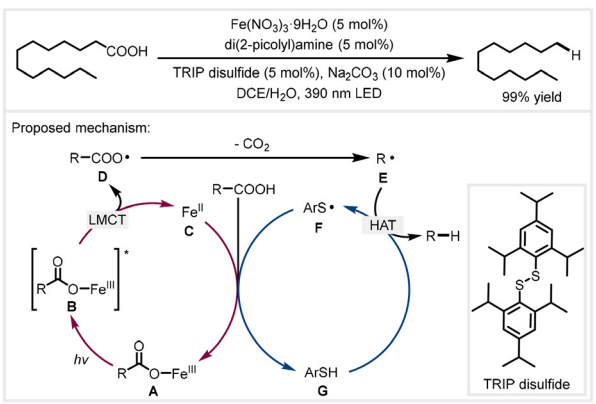

Scheme 5 Proposed mechanism for photoinduced iron/thiol dual-catalyzed decarboxylative reduction.[43] TRIP: bis(2,4,6-triisopropylphenyl). Ar: 2,4,6-triisopropylphenyl.

In recent years, some heterogeneous semiconductor TiO_2-based photocatalysts have been studied for the decarboxylative reduction of bio-derived carboxylic acids.[56–61] In 2019, Wang and co-workers found that the Pt/TiO_2 catalyst was highly active and selective for the decarboxylative reduction of bio-derived C_{12}–C_{18} fatty acids.[56] A series of various long-chain C_{n-1} alkanes could be obtained with ≥90% yields in the presence of 0.1–0.2 MPa H_2 with acetonitrile as the solvent under 365 nm LED irradiation. The authors adopted a tandem hydrogenation–decarboxylation procedure to convert industrial low-value fatty acid mixtures (such as soybean and tall oil) into C_{n-1} alkanes in high yields under mild conditions. Detailed mechanistic experimental studies revealed that the interaction between the Pt/TiO_2 photocatalyst and H_2 generated a hydrogen-rich surface that enhanced the rapid termination of alkyl radicals with the surface hydrogen species, inhibiting the formation of oligomers to improve alkane selectivity (Scheme 6).

In 2023, García, Hu, and co-workers reported that Au(core)–Pd(shell)/TiO_2 as the heterogeneous photocatalyst was found to be effective for the decarboxylative reduction of hexanoic acid.[60] This conversion showed nearly 100% selectivity toward pentane in the presence of 0.5 bar H_2, with dodecane as the solvent under 300 W Xe lamp irradiation. This catalyst system also exhibited a wide scope converting multiple long-chain fatty acids into hydrocarbons under mild conditions. After performing the reusability test five times, no obvious catalytic activity loss was observed. In addition, it could directly catalyze the transformation of raw bio-oils into C_{n-1} alkanes. The synergistic effect between Au and Pd within the nanostructured Au(core)–Pd(shell) alloy enhanced charge-separation efficiency upon visible light excitation. Based on mechanistic studies and DFT calculations, the authors proposed a reaction mechanism for decarboxylative reduction (Scheme 7). The P25 TiO_2 photocatalyst was first excited to generate photogenerated electrons and holes upon irradiation with light. Then, the carboxylate from the dissociation of the carboxylic acid was strongly adsorbed on the TiO_2 surface.

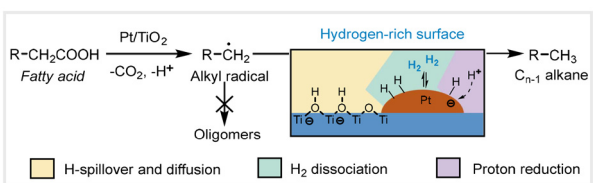

Scheme 6 Plausible reaction pathways for the photocatalytic decarboxylative reduction of fatty acids over Pt/TiO_2.[56]

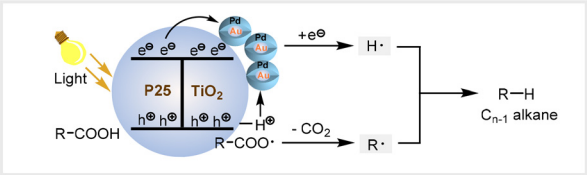

Scheme 7 The proposed mechanism for the photocatalytic decarboxylative reduction of fatty acids over a 1.5Au-0.8Pd/TiO_2 catalyst.[60]

Photogenerated holes would be quenched by the carboxyl groups to generate carboxyl radicals, which underwent rapid decarboxylation on the TiO_2 surface to generate alkyl radical species. At the same time, the protons would migrate to Au–Pd nanoparticles, combining with photogenerated electrons to form hydrogen radical species. Finally, the alkyl radical bonded with the hydrogen radical to afford C_{n-1} alkanes.

2.2 Synthesis of aliphatic amines

Aliphatic amines are versatile building blocks in a wide variety of pharmaceuticals, agrochemicals, and materials.[95] Back in 2007, Hatanaka and co-workers achieved the decarboxylative reduction of N-Boc amino acids with photogenerated cationic radicals of phenanthrene in the presence of thiols to afford N-Boc aliphatic amines.[63] However, this transformation requires stoichiometric reagents and uses high-energy UV lamps. In 2014, the Wallentin group reported a photoredox catalytic system for the decarboxylative reduction of biomass-derived α-amino and α-hydroxy acids under visible light irradiation (Scheme 8).[62] Using 1 mol% Mes-Acr-Me as the photocatalyst in combination with 10 mol% bis(4-chlorophenyl) disulfide as the co-catalyst, a wide range of aliphatic amine scaffolds could be synthesized in 1,2-dichloroethane in the presence of 20 mol% 2,6-lutidine as a base. This protocol exhibited a mild and energy-efficient system without stoichiometric additives and at low temperatures. Interestingly, regioselective decarboxylation could be achieved using differently substituted dicarboxylic acid as the substrate. In addition, the application of this approach to the decarboxylative reduction

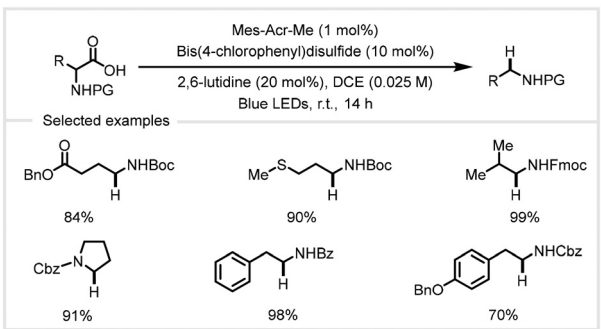

Scheme 8 Photocatalytic decarboxylative reduction of α-amino acids.[62]

of enantioenriched *N*-(1-aryl-2,2,2-trifluoroethyl) α-amino acids could give access to high value-added chiral aliphatic amines.

2.3 Synthesis of deuterated compounds

Deuterium-labeled compounds have important applications in pharmaceuticals, synthetic chemistry, and quantitative mass spectrometry.[64–66] In 2010, Yoshimi, Itou, and co-workers reported a metal-free method for decarboxylative deuteration under UV lamp irradiation.[67] In the presence of stoichiometric phenanthrene, 1,4-dicyanobenzene, and *tert*-dodecanethiol, N-Boc α-amino acids, N-protected peptides, and sugar acids were successfully decarboxylated in MeCN/D_2O mixed solvents to provide deuterated compounds in good yields with >95% D-incorporation. In 2021, Zhu, Li, Xie, and co-workers reported the catalytic decarboxylative deuteration of alkyl carboxylic acids by using Mes-Acr-MeClO_4 as the photocatalyst in combination with 2,4,6-triisopropylbenzenethiol as the co-catalyst in the presence of D_2O and a stoichiometric amount of 2,4,6-collidine.[68] Various α-amino and α-oxy carboxylic acids worked well to afford the deuterated products in good yields with high D-incorporation levels under blue LED irradiation. Moreover, the authors used a circulating reactor to achieve the gram-level synthesis of more than 10 deuterated molecules. Later, the Li group adopted a similar system to accomplish the decarboxylative deuteration of long-chain fatty acids for the synthesis of deuterated alkanes.[45] In 2024, Fu, Deng, and co-workers developed a light-induced synergistic catalytic strategy to achieve direct decarboxylative deuteration of aliphatic carboxylic acids using acridine as the photocatalyst and 4-methylthiophenol as the co-catalyst in the presence of D_2O and dichloromethane.[46] This transformation was carried out under mild conditions and required no base as additives. Biomass carboxylic acids such as levulinic acid and long-chain fatty acids worked well to afford the corresponding D-labeled products. This protocol exhibits excellent functional group tolerance. A broad range of drug molecules and natural products bearing carboxylic acid moieties were also tolerated, with a high level of D-incorporation. More importantly, a 50 mmol scale-up synthesis was achieved by using a microchannel continuous flow photoreactor that significantly improved the reaction efficiency.

In summary, the advancement of decarboxylative reduction under visible light irradiation has provided a promising space for the efficient conversion of biomass-derived carboxylic acid into biofuels and valuable chemicals, paving the way for sustainable chemical production. Although these photocatalytic systems could effectively catalyze decarboxylative reduction of carboxylic acid, there are still some problems. The production of alkane biofuels needs to consider the cost and separation energy consumption. More research should focus on the design and synthesis of photocatalysts with high catalytic decarboxylation performance and the use of green solvents such as H_2O. Given the lower tube reaction efficiency, developing continuous flow photoreactors might be a promising strategy to reduce photocatalyst usage and improve photon utilization efficiency.

3. Photochemical decarboxylative elimination

3.1 Synthesis of olefins

Olefins are one of the most versatile building blocks and are widely applied for the synthesis of polymers, surfactants, and lubricants.[69] In 2018, the Ritter group developed a synergistic catalysis strategy to accomplish the decarboxylative elimination of abundant and renewable bio-derived fatty acids to α-olefins, using 1 mol% $Ir[dF(CF_3)ppy]_2(dtbbpy)PF_6$ as the photocatalyst combined with 5 mol% $Co(dmgH)_2(4\text{-OMe-py})Cl$ as the proton reduction catalyst.[42] This transformation was carried out under mild conditions and did not require stoichiometric additives. This approach could be used for structurally more complex carboxylic acids as well, affording versatile olefin intermediates. A broad scope of functional groups including triazoles, phenols, carbonyl groups, pyridines, hydroxyl groups, and alkynyl substituents were well tolerated. It was noteworthy that the CO_2 build-up in the catalytic system has a detrimental effect on the reaction yield. A dual catalytic cycle of decarboxylative elimination was proposed, as shown in Scheme 9. Upon irradiation with visible light, photocatalyst $[Ir^{III}]$ **A** was easily accessible to generate the photoexcited $[*Ir^{III}]$ species **B** ($E_{1/2}^{red}$ ($Ir^{IV}/*Ir^{III}$) = −0.89 V *versus* SCE in MeCN). Subsequently, it would reduce the $[Co^{III}]$ catalyst **D** ($E_{1/2}^{red}$ (Co^{III}/Co^{II}) = −0.68 V *versus* SCE in MeCN) to $[Co^{II}]$ species **E**. The alkyl carboxylate **H** underwent single electron oxidation by the $[Ir^{IV}]$ species **C** ($E_{1/2}^{red}$ (Ir^{IV}/Ir^{III}) = +1.69 V *versus* SCE in MeCN) followed by decarboxylation to give alkyl radical species **I**, completing the photoredox catalyst cycle. The generated alkyl radical was then captured by the reduced $[Co^{II}]$ species **E** to furnish alkyl-$[Co^{III}]$ species **F**, which underwent photolysis to afford the corresponding olefins and $[Co^{III}]$-H species **G**. It should be noted that the formation of olefins through light-induced homolysis of the $[Co^{III}]$–C bond followed by β-hydrogen atom abstraction from the resulting $[Co^{II}]$ species is also a plausible process. Finally, the $[Co^{III}]$-H species reacted with alkyl carboxylic acid to liberate a molecule of hydrogen and regenerate the $[Co^{III}]$ catalyst.

Then in 2019, the Larionov group adopted acridine as the organophotocatalyst in combination with a cobaloxime catalyst to achieve a similar transformation.[45] The reaction was carried out in a DCM/MeCN mixed solvent under 400 nm LED irradiation for 36 hours. The advantage of this protocol was that it did not require external additives and precious metal photocatalysts. A wide variety of bio-derived carboxylic acids, pharmaceuticals, and natural products worked well to afford the corresponding functionalized terminal alkenes. This approach exhibited a cost-efficient, operationally simple, and mild system. In addition, plant oils and biomass could be directly converted into long-chain terminal alkenes *via* a triple collaboration of the chemoenzymatic lipase–acridine–cobaloxime processes. Based on detailed mechanistic experiments and DFT calculations, the authors proposed a dual acridine/cobaloxime catalytic cycle, as depicted in Scheme 10. The acridine–carboxylic acid hydrogen bonding complex **B** was formed between acridine **A** and alkyl carboxylic acids, followed by irradiation with visible light to form alkyl radicals and acridinyl radical **C** through a proton-coupled electron transfer (PCET) process. Cobaloxime catalyst **F** was reduced to the Co^{II} species **G** by the acridinyl radical **C** or photoexcited **E*** from disproportionation of the acridinyl radical, accompanied by the generation of acridinium **D**. The reaction of the alkyl radical with **G** formed alkyl-Co^{III} species **I**, and the following photoinduced homolysis afforded alkene products and $Co^{III}H$ species **H**. Finally, the $Co^{III}H$ species would react with acridinium **D** to regenerate acridine catalyst **A** and cobaloxime cata-

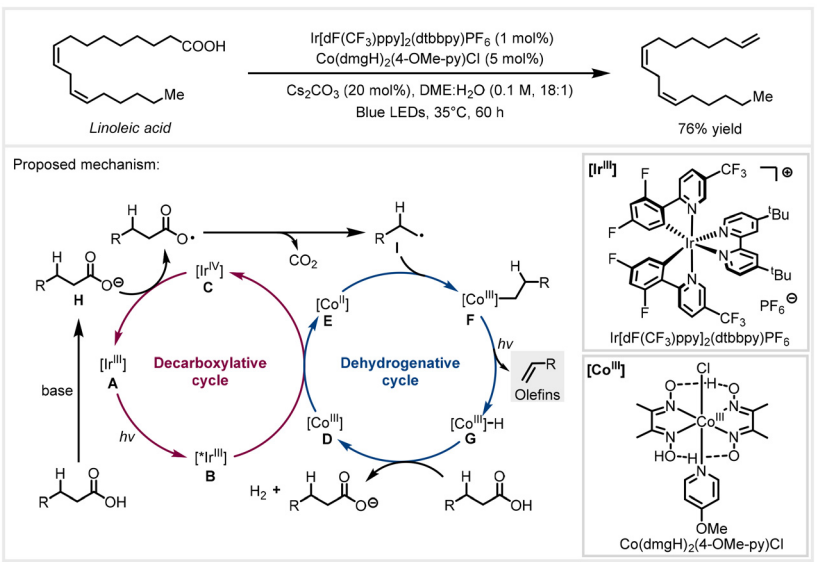

Scheme 9 Photoredox/cobalt catalyzed decarboxylative elimination of bio-derived fatty acids.[42]

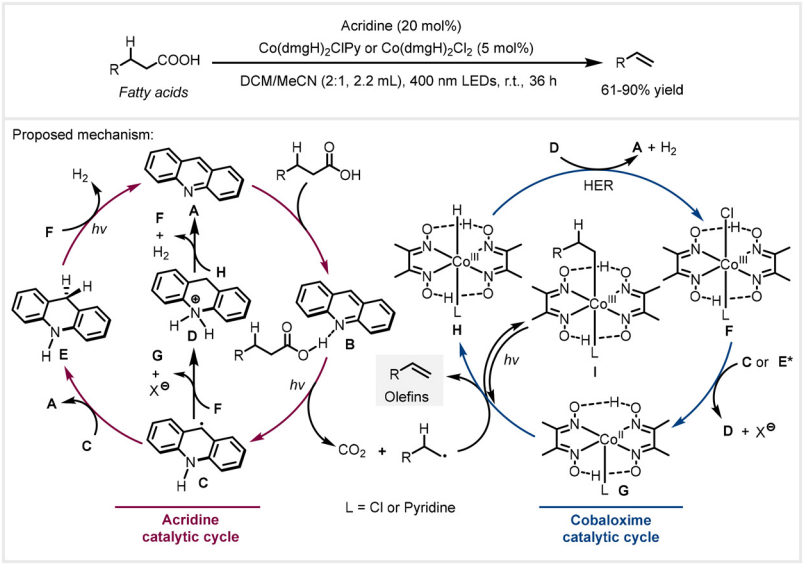

Scheme 10 Photoinduced acridine/cobalt catalyzed decarboxylative elimination of bio-derived fatty acids.[45] HER: hydrogen evolution reaction.

lyst **F**, along with the liberation of hydrogen gas, completing dual catalytic cycles. In addition, the reaction of **E** with **F** could also regenerate the acridine catalyst under visible light irradiation. It is worth noting that compared with the previous use of acridinium as the photocatalyst to oxidize aliphatic carboxylates for the formation of carboxyl radicals through single-electron transfer (SET) events, the high oxidation potential of carboxylic acids can be avoided by using the hydrogen bonding complex from acridine and the acid under light irradiation *via* proton-coupled electron transfer (PCET) in this system.

3.2 Synthesis of enamides and enecarbamates

Enamides and enecarbamates are versatile building blocks in organic synthesis that give access to complex nitrogen-containing compounds.[70] In 2018, the Tunge group reported a dual-catalytic strategy for the decarboxylative elimination of α-amino acids (Scheme 11A).[71] In the presence of 5 mol% Mes-2,7-Me_2-Acr-$PhBF_4$ as the organophotocatalyst and 3 mol% Co(dmgH)$_2$ClPy, a variety of *N*-acyl amino acids bearing alkyl or aryl substituents were successfully decarboxylated to afford the corresponding enamides and enecarbamates in MeOH/H_2O under blue LED irradiation. This transformation avoided the use of stoichiometric oxidants, toxic and expensive reagents, and harsh reaction conditions. This protocol exhibited broad functional group compatibility. In this process, sodium triacetoxyborohydride (STAB) and Na_2CO_3 served as the reductant and additive for the initial reduction of [Co^{III}] to [Co^{I}] species. Adding a small amount of water to the system could increase the product yield. It was noteworthy that the *E*/*Z* selectivity of these products was uncontrolled under these conditions. The proposed catalytic cycle is presented in Scheme 11A. The [Co^{III}] catalyst was first reduced to [Co^{I}] species **A** in the presence of STAB and Na_2CO_3. The protonation of the [Co^{I}] species

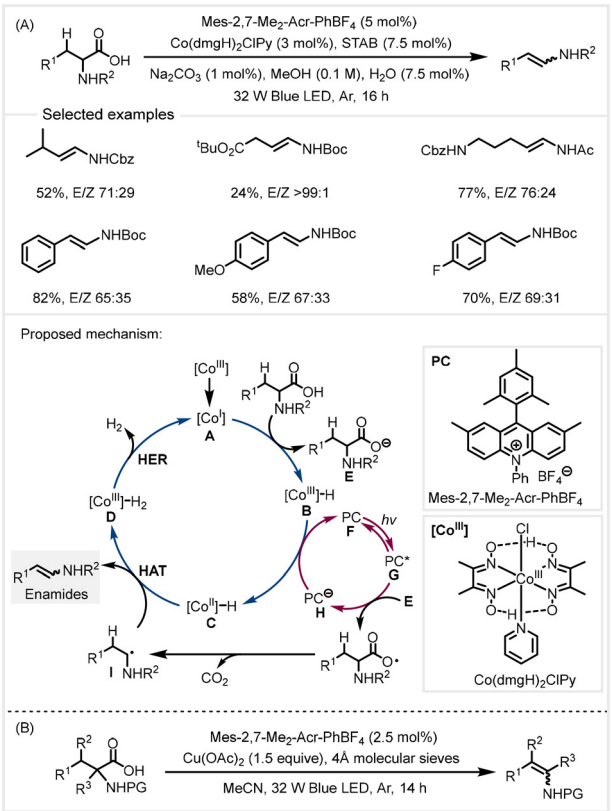

Scheme 11 Photoredox/cobalt catalyzed decarboxylative elimination of *N*-acyl α-amino acids.[71,72]

by α-amino acids formed [Co^{III}]-H species **B** and α-amino carboxylate **E**. The carbon-centered radical **I** was then generated by oxidative decarboxylation of α-amino carboxylate by photo-excited acridinium **G**. The reduced photocatalyst **H** would

reduce the [Co^{III}]-H to [Co^{II}]-H species **C** through single electron transfer events, accompanied by the regeneration of photoredox catalyst **F**. β-Hydrogen abstraction from the α-amino radical **I** by the [Co^{II}]-H species **C** provided the corresponding products and generated [Co^{III}]-H_2 species **D**, followed by hydrogen evolution to complete the cobalt catalytic cycle. Subsequently, the same group utilized 2.5 mol% Mes-2,7-Me_2-Acr-$PhBF_4$ combined with stoichiometric copper acetate to achieve the same transformation in MeCN under blue LED irradiation for 14 hours (Scheme 11B).[72] Copper acetate plays two roles in the reaction. One is to oxidize alkyl radicals to alkenes, and the other is to mediate the oxidation of acridinium to achieve a photoredox catalytic cycle.

In 2023, a similar transformation was achieved by Zeng and co-workers by using 10 mol% iron(II) acetate combined with 10 mol% $Cu(acac)_2$ under visible light irradiation (Scheme 12).[73] The key to successful transformation is that the photoexcited iron carboxylates formed from α-amino acids generate carbon-centered radicals through ligand–metal charge transfer (LMCT) events, wherein, the Cu^{II} species would capture the carbon-centered radicals to generate alkyl-Cu^{III} species, which then undergo β-hydride elimination to the corresponding products. In this system, stoichiometric di-*tert*-butyl peroxide (DTBP) was used to oxidize low-valent metal species into high-valent metal species for accomplishing a dual catalytic cycle. Deprotonation of α-amino acids by 1,8-diazabicyclo [5.4.0]undec-7-ene (DBU) formed the α-amino carboxylates that facilitated coordination with iron salts.

In summary, advancements in photocatalytic decarboxylative elimination have provided a sustainable and green approach for the efficient transformation of biomass-derived carboxylic acids to functionalized olefins, as important synthesis intermediates in organic chemistry. Nevertheless, there remains ample space for improvement in producing high-value functionalized olefins. Regardless of whether precious or organic photocatalysts are used, long reaction times are required, resulting in low production efficiency. Microchannel continuous flow reactors can enhance the photon absorption efficiency of the reaction solution *via* process intensification, thereby improving reaction efficiency. Furthermore, the *cis–trans* isomerism control over the formed olefins from the α-amino acid substrate remains elusive under these conditions.

4. Photochemical decarboxylative coupling

Light-mediated decarboxylative cross-coupling reactions can create the formation of new C–C and C–X bonds to synthesize complex functional molecules. In 2014, the MacMillan group first reported photoredox-catalyzed decarboxylative arylation, with Ir[*p*-F(*t*-Bu)-ppy]$_3$ as the photocatalyst (Scheme 13A).[74] A wide variety of benzylic amines were synthesized from renewable α-amino acids with arenes under visible light irradiation. This protocol features mild conditions and broad functional group tolerance. A photoredox catalytic cycle for direct decarboxylative arylation was proposed (Scheme 15A). Under the irradiation of light, the [Ir^{III}] photocatalyst **A** formed the excited state [*Ir^{III}] **B**. The reduction of 1,4-dicyanobenzene **D** ($E^{red}_{1/2}$ = −1.61 V *versus* SCE) by [*Ir^{III}] ($E^{red}_{1/2}$ [Ir^{IV}/*Ir^{III}] = −1.73 V

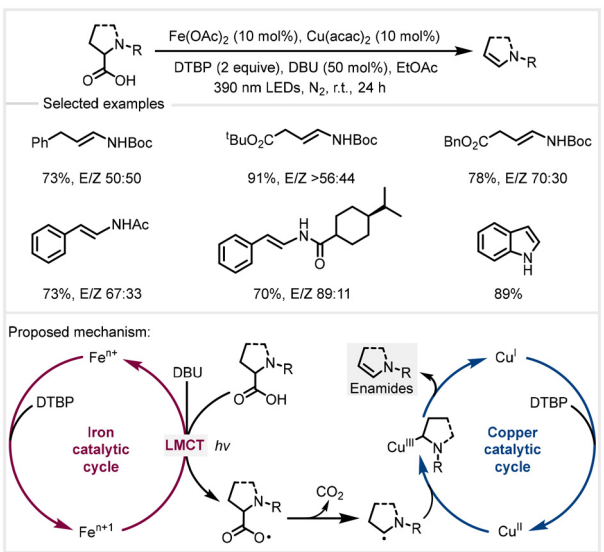

Scheme 12 Photoinduced iron/copper catalyzed decarboxylative elimination of *N*-acyl α-amino acids.[73]

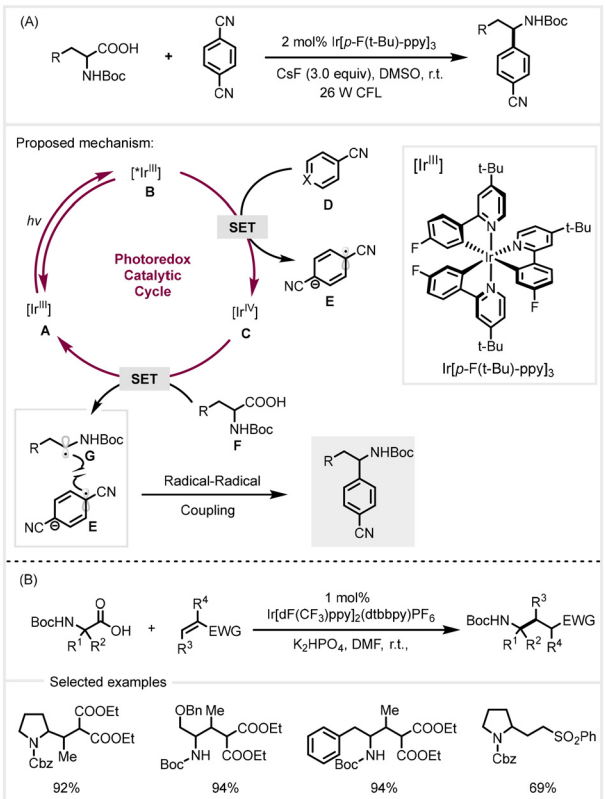

Scheme 13 Photocatalytic decarboxylative arylation and alkylation.[74,75]

versus SCE) would generate aryl radical anion **E**. Subsequent oxidation of α-amino acids by [Ir^{IV}] species **C** ($E^{red}_{1/2}$ [Ir^{IV}/Ir^{III}] = +0.77 V *versus* SCE) furnished α-amino radical **G** (upon CO_2 extrusion) and regenerated the [Ir^{III}] photocatalyst, completing the photoredox catalytic cycle. Finally, the aryl radical anion **E** coupled with the α-amino radical **G** and subsequent loss of cyanide would afford benzylic amines. Soon after that, the same group adopted a similar catalytic system to achieve radical Michael additions with α-amino acid as a free radical precursor in the presence of $Ir[dF(CF_3)ppy]_2(dtbbpy)PF_6$ as the photocatalyst (Scheme 13B).[75] A diverse array of Michael acceptors is amenable to this conjugate addition strategy. This approach exhibited broad substrate scopes and mild conditions.

In 2018, Aggarwal and co-workers adopted a similar catalytic system to accomplish the decarboxylative radical addition of α-amino acids to vinyl boronic esters.[76] With $Ir(ppy)_2(dtbbpy)PF_6$ or $Ir[dF(CF_3)ppy]_2(dtbbpy)PF_6$ as the photocatalyst, a variety of carboxylic acids and substituted alkenyl boronic esters could be converted to afford γ-amino boronic esters with good efficiency in the presence of Cs_2CO_3 (Scheme 14A). This transformation proceeded under mild photoredox catalysis and exhibited a broad scope of substrates. The same group utilized 4CzIPN as the organic photocatalyst to further realize the decarboxylative radical addition–polar cyclization cascade reaction between carboxylic acids and electron-deficient chloroalkyl alkenes (Scheme 14B).[77] A series of highly functionalized cyclopropanes could be synthesized. The mild reaction conditions were found to tolerate a wide range of functional groups on both carboxylic acids and chloroalkyl alkenes, demonstrating excellent functional group compatibility. Based on mechanistic studies, the authors proposed a catalytic cycle (Scheme 14B). Upon irradiation with visible light, the photocatalyst 4CzIPN led to the generation of the excited state PC*. Subsequent single electron oxidation of the carboxylate from deprotonation of carboxylic acids resulted in the carbon-centered radical **A** (upon CO_2 extrusion) and the reduced radical anion $PC^{\bullet-}$ ($E^{red}_{1/2}$ = −1.21 V *versus* SCE in MeCN). The carbon-centered radical underwent addition to chloroalkyl alkenes **B** to furnish the stabilized alkyl radical **C**. A single electron transfer between radical **C** ($E^{red}_{1/2}$ ≈ −0.6 V *versus* SCE in MeCN) and radical anion $PC^{\bullet-}$ would regenerate the photocatalyst, completing the photoredox catalytic cycle, and form the stabilized carbanion **D**, which then underwent a polar 3-*exo-tet* cyclization to afford the cyclopropane products.

In 2020, Aggarwal and co-workers demonstrated a three-component conjunctive cross-coupling of vinyl boronic esters with α-amino acids and aryl iodides (Scheme 15).[78] Using 4CzIPN as the photocatalyst in combination with a nickel catalyst, a range of substrates including amino acids and aryl iodides provided efficient access to highly functionalized alkyl boronic esters under visible light irradiation. This protocol features mild conditions and broad functional group tolerance. However, when other Michael acceptors were used, this protocol failed to deliver the product. The key to the success of vinyl boronic esters is a slower reduction rate of α-boryl radical by the reduced photocatalyst, which allows it to be rapidly trapped by the nickel(II) species. The proposed mechanism is depicted in Scheme 17. The carboxylate from the deprotonation of carboxylic acid with a base was oxidized by the excited photocatalyst (PC*) to generate α-amino radical **A** (upon CO_2

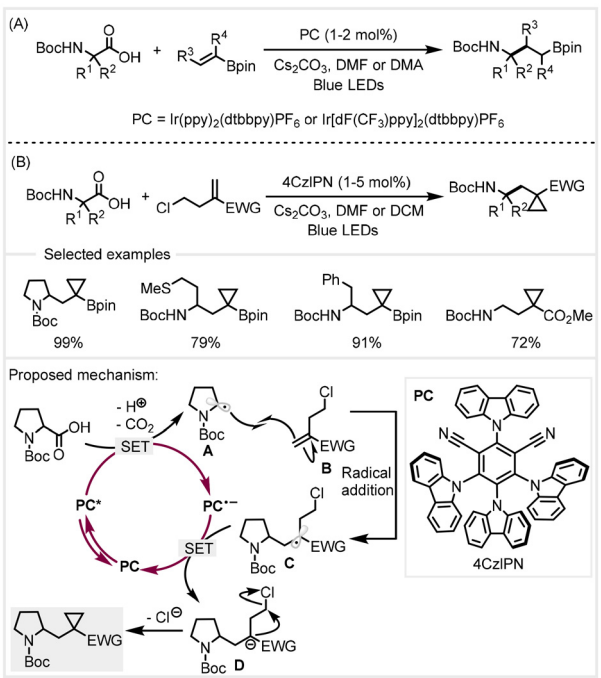

Scheme 14 Synthesis of γ-amino boronic esters and functionalized cyclopropanes from α-amino acids *via* photocatalysis.[76,77]

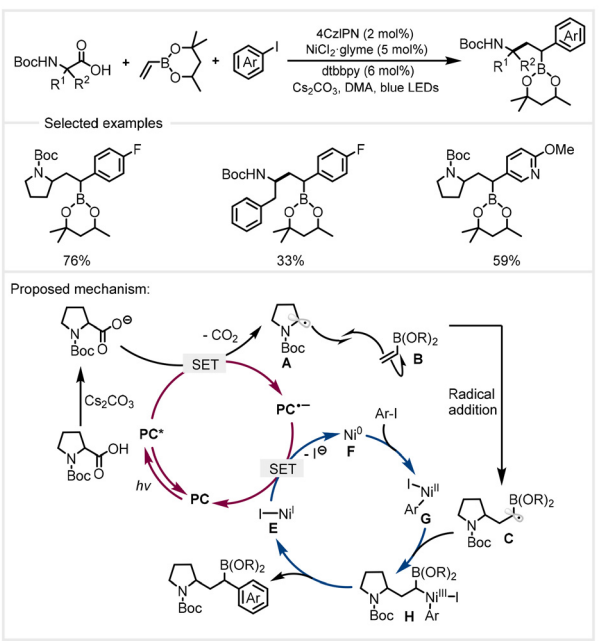

Scheme 15 Photoredox/nickel catalyzed decarboxylative conjunctive cross-coupling of vinyl boronic esters.[78]

extrusion). It would add to vinyl boronic ester **B** to generate the stabilized α-boryl radical **C**. At that stage, the oxidative addition of aryl halide to the Ni^0 species **F** formed aryl nickel (II) complex **G**. The reaction of the aryl nickel(II) complex with the α-boryl radical **C** generated nickel(III) species **H**, followed by reductive elimination to provide the product. The reduced photocatalyst ($PC^{\bullet-}$) and nickel(I) complex **E** underwent a SET to complete the two catalytic cycles.

In 2022, the Yoon group developed a metallaphotoredox strategy for the cross-selective ketonization of two structurally dissimilar carboxylic acids (Scheme 16).[79] In the presence of Boc_2O, a broad range of structurally unsymmetric ketones were prepared in moderate yields using 4CzIPN as the photocatalyst in combination with a nickel catalyst. This protocol exhibited a broad substrate scope under mild conditions. In this process, unactivated carboxylic acids underwent *in situ* acylation with di-*tert*-butyl decarbonate to enable a two-electron oxidative addition with a nickel catalyst, while another molecule of the carboxylic acid stabilized by an α-heteroatom or aryl functionality was oxidatively decarboxylated to give the stabilized carbon-centered radical. Subsequently, the formation of C–C bonds was mediated by the nickel catalyst to provide the products.

In 2018, the MacMillan group reported a photoredox/nickel catalyzed decarboxylative hydroalkylation of alkyl alkynes with carboxylic acids (Scheme 17).[80] A broad range of cyclic and α-amino/oxy acids underwent efficient coupling with 1-heptyne to afford functionalized olefins with Markovnikov regioselectivity. Alkynes containing various functional groups, such as hydroxyl, cyano, and ester groups, were tolerated. This protocol exhibited mild conditions and broad substrate scope. The authors proposed a possible dual catalytic cycle (Scheme 17). Initially, photocatalyst [Ir^{III}] **A** would generate the excited state [$*Ir^{III}$] **B** ($E_{1/2}^{red}$ [$*Ir^{III}/Ir^{II}$] = +1.21 V *versus* SCE in MeCN) upon irradiation with visible light. The photoexcited [$*Ir^{III}$] species oxidized the carboxylate from deprotonation of carboxylic acid to give alkyl radical **D**. A SET event from [Ir^{II}] species **C** to nickel(II) species **E** formed nickel(I) species **F**, which captured alkyl radicals to generate alkyl-Ni(II) species **G**. It would undergo migratory insertion coupling with alkyl

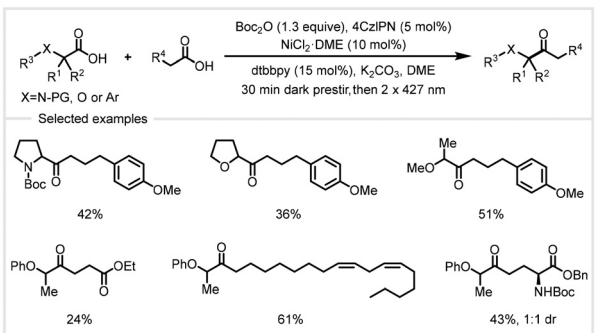

Scheme 16 Photoredox/nickel dual-catalyzed selective cross-ketonization of carboxylic acids.[79]

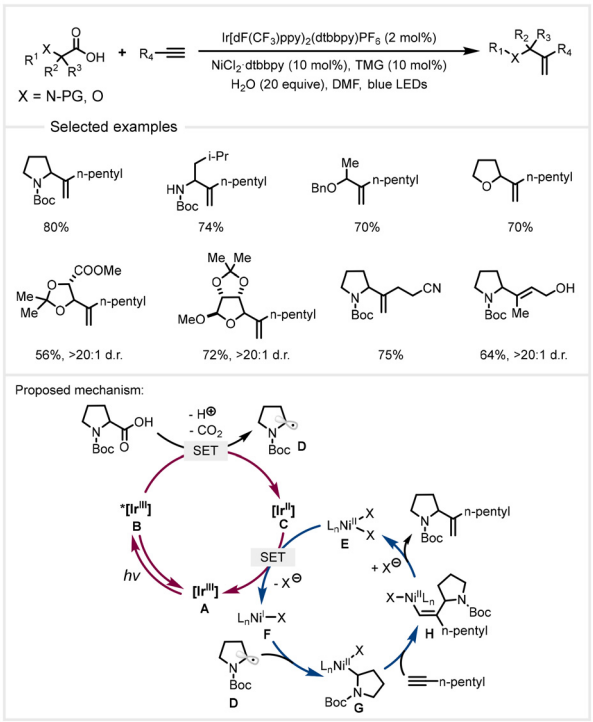

Scheme 17 Photoredox/nickel catalyzed decarboxylative hydroalkylation of alkynes.[80]

alkyne to furnish vinyl-nickel complex **H**. Finally, the protodemetalation by either a protonated base or carboxylic acid gave the final product.

In 2020, the Rueping group adopted a similar catalytic system to achieve anti-Markovnikov-type hydroalkylation of terminal arylalkynes with α-amino acids (Scheme 18A).[81] A variety of *Z*-isomer-rich disubstituted alkenes could be syn-

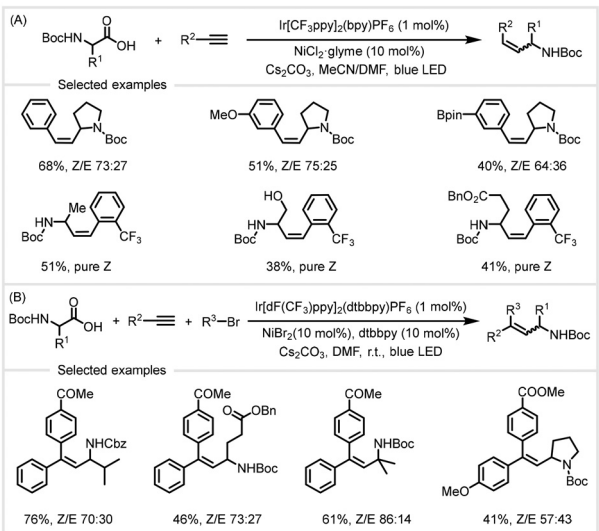

Scheme 18 Photoredox/nickel catalyzed decarboxylative hydroalkylation/arylalkylation of alkynes.[81]

thesized with moderate efficiency and excellent regioselectivity. In addition, by adjusting the reaction conditions, the authors also achieved a one-pot arylalkylation of alkynes with α-amino acids and aryl bromides through a three-component cross-coupling for the synthesis of highly valuable trisubstituted alkenes in moderate to good yields with moderate to excellent stereoselectivity (Scheme 18B). Both protocols exhibited a broad substrate scope and excellent functional group tolerance. These reactions took place under mild conditions. Mechanistic studies revealed that the conversion occurred involving a single electron transfer (SET) with subsequent energy-transfer (EnT) activation pathways.

In 2020, the Pericàs group developed a photoredox/copper dual catalysis to accomplish a similar transformation (Scheme 19).[82] The high-throughput experimentation (HTE) screening of reaction conditions revealed that tuning the combination of the ligand and base could lead to a switch in the stereochemical outcome. This protocol can be applied to the stereoselective coupling of primary, secondary, and tertiary alkyl carboxylic acids with (hetero)aromatic terminal alkynes, demonstrating broad functional group tolerance. The mechanistic experiment revealed that the *E*/*Z* selectivity of the reaction arises from an energy transfer process mediated by the 4CzIPN photocatalyst. A possible dual catalytic cycle was proposed, as shown in Scheme 19. Upon visible light irradiation, the photocatalyst 4CzIPN generated the photoexcited **PC*** species, which oxidized α-amino carboxylates from the deprotonation of carboxylic acids **D** to form carbon-centered radical species **F**. At the same time, a single electron transfer between the Cu(II) complex and $\mathbf{PC}^{\bullet-}$ yielded the Cu(I) complex. In the presence of CsOAc and alkynes, complex **A** was formed to generate the photoexcited **A*** under light irradiation, which in turn accelerated the attack of free radical **F** to form vinyl radical **B**. It would be reduced by $\mathbf{PC}^{\bullet-}$ to afford vinyl anion **C** and regenerate the photocatalyst. In the presence of AcOH, the anion species protonation and proto-demetalation of Cu–C bonds provided an *E*-isomer-rich product, which was isomerized *via* energy transfer (ET (4CzIPN) = 60 kcal mol^{-1}) to produce a *Z*-isomer product.

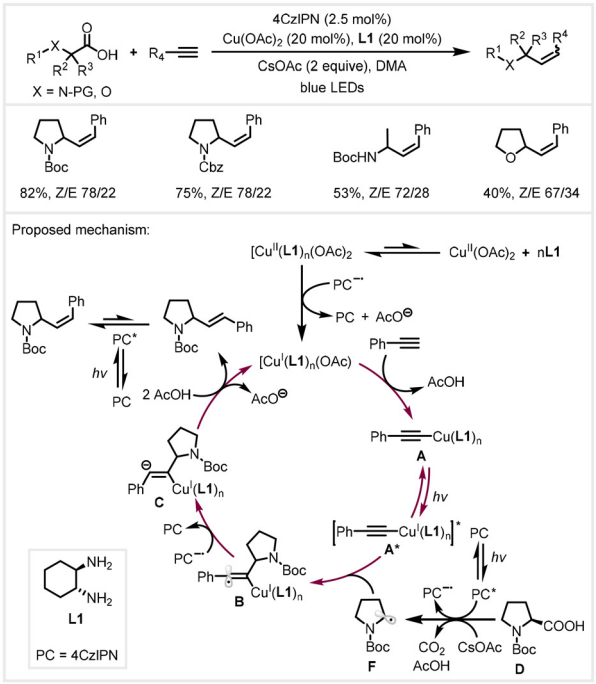

Scheme 19 Photoredox/copper catalyzed decarboxylative hydroalkylation of alkynes.[82]

In 2022, the Yoon group developed a photoinduced copper-mediated decarboxylative coupling of activated carboxylic acids with diverse nucleophiles for constructing C–C, C–O, and C–N bonds.[44] The reaction is suitable for a wide variety of coupling partners, including sulfonamides, alcohols, amides, and indoles, demonstrating broad functional group tolerance. This protocol unlocked the intrinsic photochemical reactivity of a first-row transition-metal coordination complex formed *in situ*, without an exogenous noble-metal photoredox catalyst. However, since Cu(II) is also the terminal oxidant in these reactions, it must be used stoichiometrically. Mechanistic studies revealed that visible light excitation to the ligand-to-metal charge transfer (LMCT) state resulted in a radical decarboxylation process that initiated oxidative cross-coupling. One year later, the same group achieved a similar transformation mediated by abundant, inexpensive, non-toxic iron salts under visible light irradiation.[83] In this transformation, Fe(III) serves as both the chromophore in this reaction as well as the terminal oxidant. This approach involves photochemical decarboxylation through LMCT events, followed by a radical-polar crossover process. This protocol showed mild conditions and broad functional group tolerance. Interestingly, modestly electron-rich arene nucleophiles, which gave unsatisfactory yields using the Cu(II) conditions, were excellent reaction partners using $FeCl_3$. Meanwhile, aliphatic tertiary carboxylic acids undergo only oxidative elimination to olefins under Cu(II) conditions, but they are adequate reaction partners using this protocol. It is worth noting that direct use of aliphatic amines as nucleophiles is unsuccessful in this system, possibly due to the strong binding affinity of the amines to the Lewis acidic Fe(III) center. To accomplish this transformation, another telescoped strategy by the authors is to initially obtain the chloride intermediate from the acid in the presence of $FeCl_3$ under visible light irradiation and then add amine into the system to achieve formal decarboxylative amination. This iron-mediated decarboxylative functionalization affords a blueprint for the formation of C–C, C–O, and C–N bonds from biomass carboxylic acids under photocatalysis. In the same year, the West group achieved photoinduced iron-catalyzed decarboxylative azidation from aliphatic carboxylic acids, with $TMSN_3$ as the azide source under 390 nm LED irradiation.[84] A variety of activated carboxylic acids work well with moderate to good yields. However, simple aliphatic carboxylic acids are relatively less reactive in the reaction. This protocol overcomes iron turnover and requires only catalytic amounts to achieve this transformation. Mechanistic studies demonstrated that the intrinsic oxi-

dative ability of the nitrate counterion allows the reaction to occur catalytically without an additional external oxidant.

In summary, photocatalytic decarboxylative cross-coupling of biomass-derived carboxylic acids with various coupling partners, such as aromatic halides, alkenes and terminal alkynes, have provided an efficient and sustainable protocol for constructing the C–C bond. In these photoredox systems, the photocatalyst has two functions: (1) oxidation of the carboxylate to produce free radicals and (2) reduction of electron-deficient acceptors or reduction of transition metal complexes to form low-valent active species. These photoredox/transition metal catalytic systems open up a broad space for two-component and three-component reactions to construct multiple C–C bonds. However, for the light-induced transition metal-mediated decarboxylative reaction, superstoichiometric amounts of metal salts (*e.g.*, Cu(II) and Fe(III)) are often required.[44,83] These transition metal-mediated decarboxylative functionalization offers a blueprint showing how C–N and C–O bonds might be formed from biomass carboxylic acids under photocatalysis; however, the transition metal turnover has not been demonstrated, representing a remaining opportunity for photocatalysis design.

5. Electrochemical decarboxylative coupling

In 2012, Schröder *et al.* adopted electrochemical reduction combined with oxidative Kolbe electrolysis for the conversion of biomass-derived levulinic acid into octane biofuel *via* two steps (Scheme 20A).[85] This reaction featured mild conditions and high selectivity (up to 97.2%) and used H_2O as the solvent. In this transformation, levulinic acid was reduced to generate valeric acid intermediates in sulfuric acid aqueous solution at a current density of 20–40 mA cm^{-2}. The valeric acid underwent oxidative decarboxylation on the anode surface to generate alkyl radicals in methanolic KOH solution at a current density of 15–20 mA cm^{-2}, which further would undergo radical–radical homocoupling to obtain the octane product. Since the reaction takes place in the aqueous phase, the alkane products can be easily separated from the reaction system. Owing to the inconsistency of the two-step conditions, the intermediate valeric acid needs to be separated in this system. Further research is needed to unify the composition of the electrolytes for the anode and cathode reactions to eliminate the intermediate isolation steps. In the same year, Yuan *et al.* reported the electrochemical reformation of biomass-derived levulinic acid in a MeOH/H_2O system into 5-acetyl-2,9-decanedione at a current density of 25–40 mA cm^{-2} in an undivided cell (Scheme 20B).[86] The addition of H_2O into the reaction system is crucial for the formation of the product. The authors proposed that the formation of 5-acetyl-2,9-decanedione was *via* a side reaction of Kolbe electrolysis. In 2017, Mascal and co-workers adopted Kolbe electrolysis to achieve homocoupling of biomass-derived acids in a methanolic KOH solution (Scheme 20C and D).[87] Using platinum plate electrodes in an undivided cell at a current density of 178 mA cm^{-2}, levulinic acid could be directly converted into 2,7-octanedione in 65% yield at 90% conversion. Using 2,7-octanedione as a precursor, acid-catalyzed intramolecular aldol condensation was performed followed by a hydrodeoxygenation reaction to obtain branched cycloalkane fuels. Analogous electrolysis of 2-methylsuccinic acid 1-methyl ester from biomass-derived itaconic acid could obtain 2,5-dimethyladipic acid diester in 60% yield with 85% conversion at a current density of 180 mA cm^{-2} across platinum electrodes in an undivided cell (Scheme 20D).[87]

In 2023, Baran and co-workers developed a waveform-controlled electrolysis that addressed the limitations of the Kolbe coupling reaction due to its poor chemoselectivity and reliance on noble metal electrodes (Scheme 21).[88] In this transformation, employing a square wave with an optimal frequency of 50 ms for the alternating current was essential. Using 10 mol% $Me_4N{\cdot}OH$ as the additive and acetone as the solvent

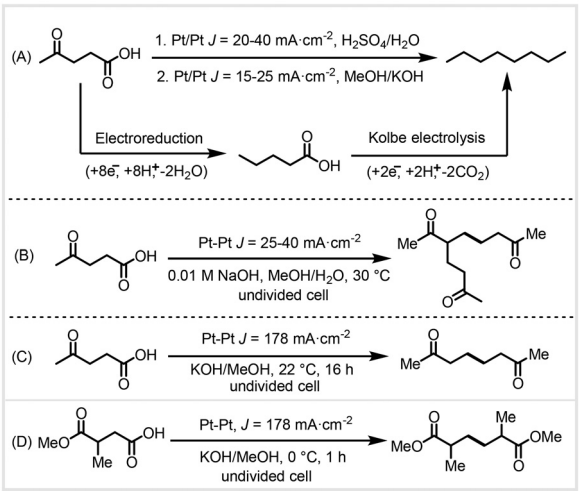

Scheme 20 Electrochemical homocoupling of biomass carboxylic acids.[85–87]

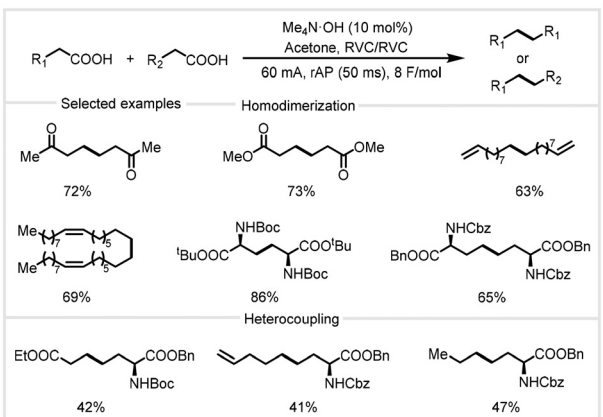

Scheme 21 rAP-Kolbe coupling reaction of biomass carboxylic acids.[88]

at a current of 60 mA, a broad range of biomass-derived aliphatic carboxylic acids could be efficiently decarboxylated to obtain the homodimerization products in good yields. The use of rapid alternating polarity (rAP) imparts good functional group tolerance, including esters, carbamates, hydroxyls, ketones, electron-deficient and electron-rich aromatics, and terminal and internal olefins. This approach is also amenable to heterocoupling to synthesize valuable unnatural amino acids from inexpensive natural amino acids with another aliphatic carboxylic acid. Using biomass-derived levulinic acid as the feedstock, a 300 mmol scale-up reaction occurred smoothly to provide the 2,7-octanedione product in 43% isolated yield, without the need to completely isolate air and moisture, demonstrating excellent industrial application potential. This protocol allows the use of cheap and sustainable carbon-based electrodes (amorphous carbon) to replace expensive platinum electrodes used in traditional Kolbe electrolysis. Mechanistic studies revealed that the waveform plays an important role in regulating the local pH around the electrode, and acetone, as an unconventional solvent, acts as an electron donor and proton acceptor in the reaction.

In summary, electrocatalytic decarboxylative homo-coupling or cross-coupling of biomass-derived carboxylic acids has afforded an efficient and sustainable strategy for manufacturing biofuels and bio-based material monomers. Although some progress has been made, there is still much to explore. Currently, these electrodes require the use of precious metal Pt electrodes. Since the reserves of precious metals are limited, the development of cheap and sustainable electrodes is a good alternative. In addition, the carboxylate is prone to over-oxidation on platinum electrodes for the formation of carbocation intermediates (Hofer–Moest reactivity), resulting in poor selectivity. More research focusing on electrode materials and electrode surface environment may become the key to solving over-oxidation. For biomass-derived levulinic acid, the one-pot two-step conversion to alkane remains difficult due to the need to consider the compatibility of the two-step process between electroreduction and homo-coupling.

6. Electrochemical decarboxylative oxidation

In 2012, Fu and co-workers developed an electrochemical route for the production of adiponitrile from biomass-derived glutamic acid under mild conditions.[89] This conversion includes (1) mono-esterification of glutamic acid, (2) electrooxidative decarboxylation to 3-cyanopropanoic acid methyl ester, and (3) Kolbe-coupling reactions of 3-cyanopropanoic acid methyl ester (Scheme 22). In the presence of sodium bromide, electrolysis of glutamic acid 5-methylester led to decarboxylative oxidation in MeOH/H_2O at a current density of 80 mA cm^{-2} across platinum electrodes, giving 3-cyanopropanoic acid methyl ester in 91% yield. Sodium bromide acts as both supporting electrolytes and mediators in anodic oxidations. Treatment of 3-cyanopropanoic acid methyl ester with

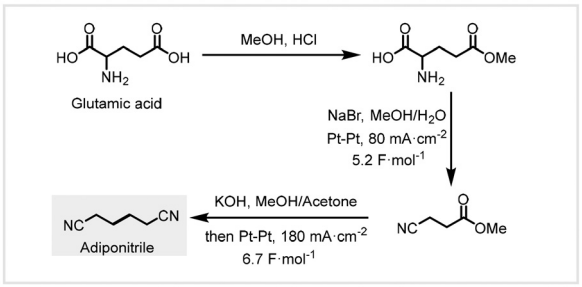

Scheme 22 Electrochemical routes for the synthesis of adiponitrile from biomass-derived glutamic acid.[89]

KOH in methanol obtained potassium 3-cyanopropanoate, and then addition of acetone as the co-solvent for Kolbe electrolysis at a current density of 180 mA cm^{-2} was performed to furnish adiponitrile in 78% yield. The authors conducted a 20 mmol scale-up reaction to provide adiponitrile from biomass-derived glutamic acid in 58% overall yield, further demonstrating the practicality of this protocol.

After two years, De Vos and co-workers reported a bromide-assisted electrochemical decarboxylation for the extension of the scope of amino acids (Scheme 23).[90] With the Pt electrode

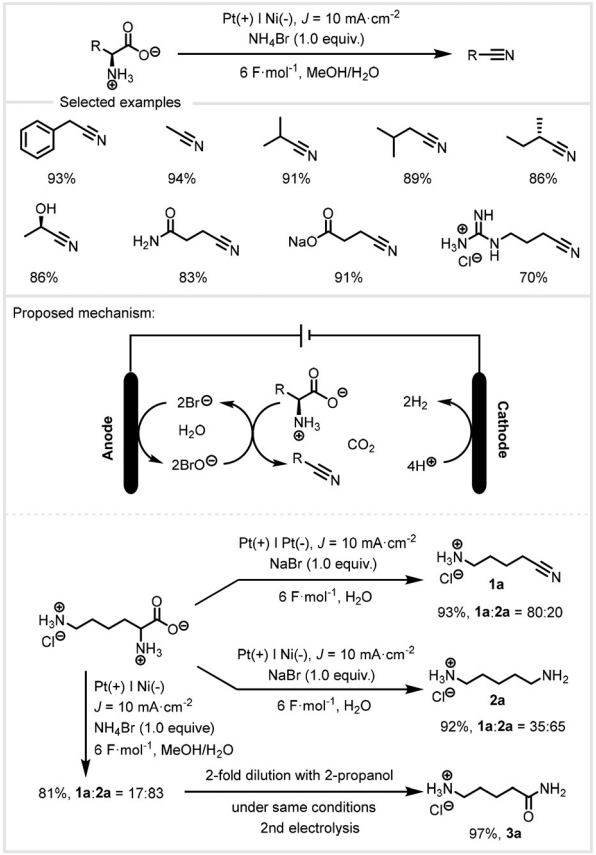

Scheme 23 Electrochemical decarboxylation of α-amino acids to nitriles.[90]

as the anode and the Ni electrode as the cathode at a current density of 10 mA cm^{-2}, various nitriles could be synthesized in $MeOH/H_2O$, affording high yields with excellent regioselectivity. In this reaction, bromide salts serve as both redox mediators and supporting electrolytes. This protocol features mild conditions and good functional group compatibility. A wide range of functional groups such as phenyl, hydroxyl and amide are tolerated. Interestingly, lysine monohydrochloride could be selectively decarboxylated in the reaction. Depending on the cathode material, the selectivity could be shifted towards nitrile **1a** or amine **2a**. For nickel anode materials, nitrile hydrogenation was preferred in this system. Moreover, after full conversion of the amino acid, the reaction mixture with 2-propanol dilution and further electrolysis could be almost quantitatively converted into 5-aminopentanamide monohydrochloride **3a**.

In 2019, Wang, Echavarren, and co-workers developed an electrochemical oxidation for the construction of C–N bonds (Scheme 24).[91] With benzimidazole as the nucleophile, various α-amino acids could be converted into N-containing compounds in the presence of $^{n}Bu_4NPF_6$ at a current of 7 mA in an undivided cell. This protocol avoided the preactivation of carboxylic acids and the use of external oxidants. In addition to benzimidazole, a range of N-nucleophiles including pyrazole, 1,2,3- and 1,2,4-triazole, benzotriazole, and tetrazole derivatives were found to be efficient, affording the corresponding products in good yields with excellent regioselectivity. Adding $BF_3{\cdot}Et_2O$ to the system, Boc-L-glutamine underwent intramolecular reaction through electrolysis to give the cyclized product in 60% yield. This transformation proceeds *via* anodic oxidative decarboxylation for the generation of stable carbocation, which is then trapped by N-nucleophiles to provide cross-coupling products.

In the same year, Wang and co-workers developed a tandem electrosynthesis of ethyl 2-(quinolin-2-yl) acetate with α-amino acids (Scheme 25).[92] In the presence of *n*-Bu_4NI and $NaHCO_3$ in MeCN, a variety of 1,3-disubstituted imidazo[1,5-*a*]-quinolines could be synthesized with two Pt electrodes in an undivided cell. Based on mechanistic experiments and previous reports, the authors proposed a possible reaction mechanism

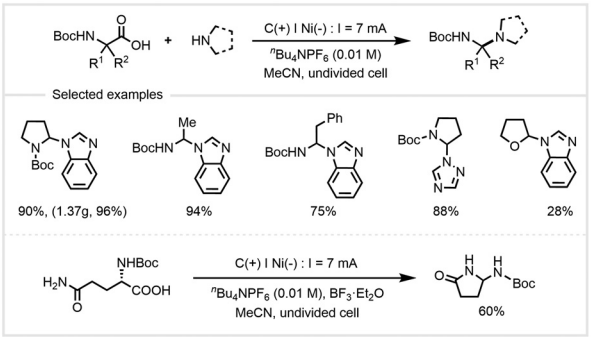

Scheme 24 Electrochemical decarboxylation of α-amino acids for the formation of C–N bonds.[91]

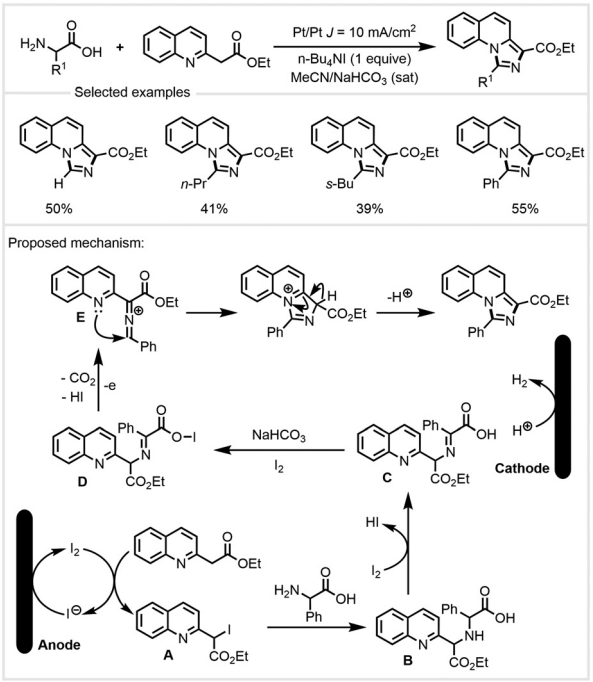

Scheme 25 Electrosynthesis of 1,3-disubstituted imidazo[1,5-*a*]quinolines from α-amino acids.[92]

(Scheme 25). The iodine anion was oxidized at the anode to produce molecular iodine. It reacted with ethyl 2-(quinolin-2-yl)acetate to generate iodinated intermediate **A**. The reaction of intermediate **A** with phenylglycine produced intermediate **B**, which was oxidized by molecular iodine to yield intermediate **C** and release a molecule of HI. In the presence of I_2 and $NaHCO_3$, it would be converted into intermediate **D**, which then further underwent a tandem cyclization process to form the final products.

In 2023, Baran and co-workers developed an electrochemical decarboxylative olefination from free carboxylic acids without preactivation under alternating polarity.[93] The authors achieved chemoselective Hofer–Moest reactivity (oxidative decarboxylation to generate carbocations) on conventionally difficult carboxylic acid substrates by modulating electrode surface quality and local acidity. This protocol avoided the need for expensive catalysts, ligands, metals, and additives. The facile execution of the kilogram scale reaction was accomplished, demonstrating the application potential of this electrochemical reaction. However, this electrochemical reaction has certain limitations for substrates with reductively labile functionality. For example, alkyl halides, aryl sulfonamides, electron-poor heterocycles, or enones were not amenable to the presented conditions. In addition, tertiary alkyl amines or electron-rich heterocycles could also interfere with oxidative decarboxylation.

Overall, advancements in electrocatalytic decarboxylative oxidation have furnished a green and efficient method for producing high value-added nitriles, amines and heterocyclic compounds from bio-derived amino acids. The application

value of these carboxylic acids is greatly improved *via* an electrocatalysis strategy. Electrochemical decarboxylative oxidation can avoid the use of stoichiometric oxidants and make the reaction process cleaner and greener. However, compounds containing functional groups that are susceptible to oxidation often have poor tolerance under these conditions. Therefore, milder electrochemical reaction conditions need to be developed. These electrocatalysis protocols afford a good way to achieve high-value utilization of biomass in the sustainable chemical transformation.

7. Conclusions and outlook

In this review, we have summarized the recent progress in the photochemical and electrochemical direct decarboxylative conversion of biomass-derived alkyl carboxylic acids for the production of biofuels and high-value chemicals in a sustainable manner. Compared to traditional thermocatalysis, these photo- and electrochemical reactions exhibited mild conditions and broad functional group tolerance. A broad range of valuable compounds such as alkanes, alkenes, amides, enamines, borate esters, ketones, nitriles, and heterocycles were prepared. These successful examples provide broad potential for the green, efficient, and sustainable transformation of renewable resources. Additionally, the discussions encompassed the mechanistic aspects of these transformations.

Despite significant progress being made in the conversion of bio-based aliphatic carboxylic acids through photochemical or electrochemical strategies, there are still challenges that need to be addressed.

In terms of photocatalytic decarboxylation, the synthesis of alkanes predominantly operates on a laboratory scale and still has a long way to achieve industrial production. The design and utilization of a continuous-flow photocatalytic reactor can help accelerate photochemical reactions to achieve this goal. For the production of biofuels, the use of a greener single solvent system (such as H_2O) can effectively reduce separation energy consumption of products and simplify post-treatment processes. Given the high cost and large usage of current photocatalysts, developing inexpensive, efficient and recyclable photocatalysts is essential for sustainable chemistry. Furthermore, most photocatalytic systems require the deprotonation of carboxylic acids with bases to form the carboxylate, resulting in the generation of large amounts of wastes. Further research can focus on developing new activation modes of carboxylic acids.

In terms of electrocatalytic decarboxylation, the current use of electrodes still mainly relies on the precious metal Pt. Since precious metals are expensive and have limited reserves, future research should focus more on the development of cheap and sustainable electrodes such as carbon electrodes. In addition, these catalytic systems use direct current in the reaction, and attempts to perform these reactions using alternating current may provide new reaction pathways.

For photo- or electrocatalysis, whether the reaction process is green and whether it reduces carbon emissions cannot be simply used as a single indicator. Instead, a more systematic and comprehensive assessment method for this process is needed, such as life cycle assessment (LCA).[94] Starting from bio-based aliphatic carboxylic acids as key building blocks, asymmetric decarboxylative reactions mediated by light or electricity for constructing high value-added chiral molecules are relatively underdeveloped. Future work can focus on developing chiral catalysts that are applicable under these photochemical and electrochemical conditions and understanding the mechanism of stereoselectivity control. The selective decarboxylative cross-coupling between two free alkyl carboxylic acids has not yet been achieved, and further development of the combination of photochemistry and electrochemistry might be a good solution.

Author contributions

Chen-Qiang Deng: conceptualization and writing – original draft. Jin Deng: conceptualization, funding acquisition, supervision, and writing – review & editing.

Data availability

No primary research results, software or code have been included and no new data were generated or analysed as part of this review.

Conflicts of interest

There are no conflicts to declare.

Acknowledgements

This work was supported by the National Natural Science Foundation of China (22478374 and 22279125).

References

1 N. Dahmen, I. Lewandowski, S. Zibek and A. Weidtmann, *GCB Bioenergy*, 2019, **11**, 107–117.
2 V. Ashokkumar, R. Venkatkarthick, S. Jayashree, S. Chuetor, S. Dharmaraj, G. Kumar, W.-H. Chen and C. Ngamcharussrivichai, *Bioresour. Technol.*, 2022, **344**, 126195.
3 Z. Zhang, J. Song and B. Han, *Chem. Rev.*, 2017, **117**, 6834–6880.
4 C.-H. Zhou, X. Xia, C.-X. Lin, D.-S. Tonga and J. Beltramini, *Chem. Soc. Rev.*, 2011, **40**, 5588–5617.
5 B. M. Upton and A. M. Kasko, *Chem. Rev.*, 2016, **116**, 2275–2306.
6 W. Deng, Y. Feng, J. Fu, H. Guo, Y. Guo, B. Han, Z. Jiang, L. Kong, C. Li, H. Liu, P. T. T. Nguyen, P. Ren, F. Wang,

S. Wang, Y. Wang, Y. Wang, S. S. Wong, K. Yan, N. Yan, X. Yang, Y. Zhang, Z. Zhang, X. Zeng and H. Zhou, *Green Energy Environ.*, 2023, **8**, 10–114.
7 C. O. Tuck, E. Perez, I. T. Horváth, R. A. Sheldon and M. Poliakoff, *Science*, 2012, **337**, 695–699.
8 G. Zhu, M. Zhu, E. Wang, C. Gong, Y. Wang, W. Guo, G. Xie, W. Chen, C. He, L. Xu, Y. Zhang, H. Li and Z. Fang, *Chem. Eng. J.*, 2024, **486**, 150195.
9 Z. Sun, G. Bottari, A. Afanasenko, M. C. A. Stuart, P. J. Deuss, B. Fridrich and K. Barta, *Nat. Catal.*, 2018, **1**, 82–92.
10 X. Wu, X. Fan, S. Xie, J. Lin, J. Cheng, Q. Zhang, L. Chen and Y. Wang, *Nat. Catal.*, 2018, **1**, 772–780.
11 J. Gao, W. Yu, Y. Li, M. Jin, L. Yao and Y. J. Zhou, *Nat. Chem. Biol.*, 2023, **19**, 1524–1531.
12 L. Xu, Z. He, H. Zhang, S. Wu, C. Dong and Z. Fang, *Bioresour. Technol.*, 2021, **320**, 124252.
13 L. Deng, J. Li, D. M. Lai, Y. Fu and Q. X. Guo, *Angew. Chem., Int. Ed.*, 2009, **48**, 6529–6532.
14 C.-Q. Deng, J. Liu, J.-H. Luo, L.-J. Gan, J. Deng and Y. Fu, *Angew. Chem., Int. Ed.*, 2022, **61**, e2021159.
15 P. Bhaumik and P. L. Dhepe, *ACS Catal.*, 2013, **3**, 2299–2303.
16 X. Wang, Y. Song, C. Huang, F. Liang and B. Chen, *Green Chem.*, 2014, **16**, 4234–4240.
17 W. Deng, P. Wang, B. Wang, Y. Wang, L. Yan, Y. Li, Q. Zhang, Z. Cao and Y. Wang, *Green Chem.*, 2018, **20**, 735–744.
18 Y. Tashinoa and H. Togo, *Synlett*, 2004, 2010–2012.
19 Q. Sun, S. Wang and H. Liu, *ACS Catal.*, 2019, **9**, 11413–11425.
20 Y. N. Palai, A. Shrotri and A. Fukuoka, *ACS Catal.*, 2022, **12**, 3534–3542.
21 X.-L. Li, K. Zhang, J.-L. Jiang, R. Zhu, W.-P. Wu, J. Deng and Y. Fu, *Green Chem.*, 2018, **20**, 362–368.
22 M. J. Haas, *Fuel Process. Technol.*, 2005, **86**, 1087–1096.
23 N. Z. A. Kapor, G. P. Maniam, M. H. A. Rahim and M. M. Yusoff, *J. Cleaner. Prod.*, 2017, **143**, 1–9.
24 H. Yan, M. Zhao, X. Feng, S. Zhao, X. Zhou, S. Li, M. Zha, F. Meng, X. Chen, Y. Liu, D. Chen, N. Yan and C. Yang, *Angew. Chem., Int. Ed.*, 2022, **61**, e202116059.
25 C.-Q. Deng, J. Deng and Y. Fu, *Green Chem.*, 2022, **24**, 8477–8483.
26 S. Song, J. Qu, P. Han, M. J. Hülsey, G. Zhang, Y. Wang, S. Wang, D. Chen, J. Lu and N. Yan, *Nat. Commun.*, 2020, **11**, 4899.
27 Y.-W. Han, L. Ye, T.-J. Gong and Y. Fu, *Angew. Chem., Int. Ed.*, 2023, **62**, e2023063.
28 R. W. Gosselink, S. A. W. Hollak, S.-W. Chang, J. van Haveren, K. P. de Jong, J. H. Bitter and D. S. van Es, *ChemSusChem*, 2013, **6**, 1576–1594.
29 Z. Zhang, Z. Chen, H. Chen, X. Gou, K. Chen, X. Lu, P. Ouyang and J. Fu, *Sustainable Energy Fuels*, 2018, **2**, 1837–1843.
30 N. Rodríguez and L. J. Goossen, *Chem. Soc. Rev.*, 2011, **40**, 5030–5048.
31 M.-C. Fu, R. Shang, B. Zhao, B. Wang and Y. Fu, *Science*, 2019, **363**, 1429–1434.
32 X. Wu, N. Luo, S. Xie, H. Zhang, Q. Zhang, F. Wang and Y. Wang, *Chem. Soc. Rev.*, 2020, **49**, 6198–6223.
33 Z. Huang, N. Luo, C. Zhang and F. Wang, *Nat. Rev. Chem.*, 2022, **6**, 197–214.
34 X. Wu, S. Xie, H. Zhang, Q. Zhang, B. F. Sels and Y. Wang, *Adv. Mater.*, 2021, **33**, 2007129.
35 T. Liu, J. Huang, J. Li, K. Wang, Z. Guo, H. Wu, S. Yang and H. Li, *Green Chem.*, 2023, **25**, 10338–10365.
36 W.-M. Zhang, K.-W. Feng, R.-G. Hu, Y.-J. Guo and Y. Li, *Chem*, 2023, **9**, 430–442.
37 S. A. Akhade, N. Singh, O. Y. Gutiérrez, J. Lopez-Ruiz, H. Wang, J. D. Holladay, Y. Liu, A. Karkamkar, R. S. Weber, A. B. Padmaperuma, M.-S. Lee, G. A. Whyatt, M. Elliott, J. E. Holladay, J. L. Male, J. A. Lercher, R. Rousseau and V.-A. Glezakou, *Chem. Rev.*, 2020, **120**, 11370–11419.
38 J. Wu, L. Xu, Y. Li, C.-L. Dong, Y. Lu, T. T. T. Nga, Z. Kong, S. Li, Y. Zou and S. Wang, *J. Am. Chem. Soc.*, 2022, **144**, 23649–23656.
39 D. Saha, *Chem. – Asian J.*, 2020, **15**, 2129–2152.
40 J. D. Griffin, M. A. Zeller and D. A. Nicewicz, *J. Am. Chem. Soc.*, 2015, **137**, 11340–11348.
41 Y.-L. Sun, F.-F. Tan, R.-G. Hu, C.-H. Hu and Y. Li, *Chin. J. Chem.*, 2022, **40**, 1903–1908.
42 X. Sun, J. Chen and T. Ritter, *Nat. Chem.*, 2018, **10**, 1229–1233.
43 Y.-C. Lu and J. G. West, *Angew. Chem.*, 2023, **135**, e202213055.
44 Q. Y. Li, S. N. Gockel, G. A. Lutovsky, K. S. DeGlopper, N. J. Baldwin, M. W. Bundesmann, J. W. Tucker, S. W. Bagley and T. P. Yoon, *Nat. Chem.*, 2022, **14**, 94–99.
45 V. T. Nguyen, V. D. Nguyen, G. C. Haug, H. T. Dang, S. Jin, Z. Li, C. Flores-Hansen, B. S. Benavides, H. D. Arman and O. V. Larionov, *ACS Catal.*, 2019, **9**, 9485–9498.
46 C.-Q. Deng, Y. Xu, J.-H. Luo, G.-Z. Wang, J. Deng and Y. Fu, *Chem. Catal.*, 2024, **4**, 100899.
47 J. G. L. de Araujo, M. D. S. B. da Silva, J. C. C. V. Bento, A. M. de Azevêdo, A. M. D. M. Araújo, A. S. D. dos Anjos, C. A. Martínez-Huitle, E. V. dos Santos, A. D. Gondim and L. N. Cavalcanti, *Chem. – Eur. J.*, 2023, **29**, e202302330.
48 S. Möhle, M. Zirbes, E. Rodrigo, T. Gieshoff, A. Wiebe and S. R. Waldvogel, *Angew. Chem., Int. Ed.*, 2018, **57**, 6018–6041.
49 B. A. Frontana-Uribe, R. D. Little, J. G. Ibanez, A. Palmad and R. Vasquez-Medranoc, *Green Chem.*, 2010, **12**, 2099–2119.
50 H. Kolbe, *Justus Liebigs Ann. Chem.*, 1848, **64**, 339–334.
51 J. Xuan, Z.-G. Zhang and W.-J. Xiao, *Angew. Chem., Int. Ed.*, 2015, **54**, 15632–15641.
52 J. Schwarz and B. König, *Green Chem.*, 2018, **20**, 323–361.
53 S. B. Beil, T. Q. Chen, N. E. Intermaggio and D. W. C. MacMillan, *Acc. Chem. Res.*, 2022, **55**, 3481–3494.
54 V. Ramadoss, Y. Zheng, X. Shao, L. Tian and Y. Wang, *Chem. – Eur. J.*, 2021, **27**, 3213–3228.
55 T. S. Mayer, T. Taeufer, S. Brandt, J. Rabeah and J. Pospech, *J. Org. Chem.*, 2023, **88**, 6347–6353.

56 Z. Huang, Z. Zhao, C. Zhang, J. Lu, H. Liu, N. Luo, J. Zhang and F. Wang, *Nat. Catal.*, 2020, **3**, 170–178.
57 Y. Fan, X. Qin, Y. Zhai, Z. Huang, Z. Wu, M. Tan, J. Deng, Y. Zhu and H. Li, *Biomass Bioenergy*, 2022, **167**, 106649.
58 X. Du, Y. Peng, J. Albero, D. Li, C. Hu and H. García, *ChemSusChem*, 2022, **15**, e2021021.
59 Z. Huang, Y. Yang, J. Mu, G. Li, J. Han, P. Ren, J. Zhang, N. Luo, K.-L. Han and F. Wang, *Chin. J. Catal.*, 2023, **45**, 120–131.
60 H. Yang, L. Tian, A. Grirrane, A. García-Baldoví, J. Hu, G. Sastre, C. Hu and H. García, *ACS Catal.*, 2023, **13**, 15143–15154.
61 K. Liu, A. Litke, Y. Su, B. G. van Campenhout, E. A. Pidko and E. J. M. Hensen, *Chem. Commun.*, 2016, **52**, 11634–11637.
62 C. Cassani, G. Bergonzini and C.-J. Wallentin, *Org. Lett.*, 2014, **16**, 4228–4231.
63 Y. Yoshimi, T. Itou and M. Hatanaka, *Chem. Commun.*, 2007, 5244–5246.
64 C. Schmidt, *Nat. Biotechnol.*, 2017, **35**, 493–494.
65 M. Gómez-Gallego and M. A. Sierra, *Chem. Rev.*, 2011, **111**, 4857–4963.
66 D. H. Chace, T. Lim, C. R. Hansen, B. W. Adam and W. H. Hannon, *Clin. Chim. Acta*, 2009, **402**, 14–18.
67 T. Itou, Y. Yoshimi, K. Nishikawa, T. Morita, Y. Okada, N. Ichinose and M. Hatanaka, *Chem. Commun.*, 2010, 6177–6179.
68 N. Li, Y. Ning, X. Wu, J. Xie, W. Li and C. Zhu, *Chem. Sci.*, 2021, **12**, 5505–5510.
69 K. D. Nguyen, B. Y. Park, T. Luong, H. Sato, V. J. Garza and M. J. Krische, *Science*, 2016, **354**, aah5133.
70 R. Matsubara and S. Kobayashi, *Acc. Chem. Res.*, 2008, **41**, 292–301.
71 K. C. Cartwright and J. A. Tunge, *ACS Catal.*, 2018, **8**, 11801–11806.
72 K. C. Cartwright, S. B. Lang and J. A. Tunge, *J. Org. Chem.*, 2019, **84**, 2933–2940.
73 N. Xiong, Y. Li and R. Zeng, *ACS Catal.*, 2023, **13**, 1678–1685.
74 Z. Zuo and D. W. C. MacMillan, *J. Am. Chem. Soc.*, 2014, **136**, 5257–5260.
75 L. Chu, C. Ohta, Z. Zuo and D. W. C. MacMillan, *J. Am. Chem. Soc.*, 2014, **136**, 10886–10889.
76 A. Noble, R. S. Mega, D. Pflästerer, E. L. Myers and V. K. Aggarwal, *Angew. Chem., Int. Ed.*, 2018, **57**, 2155–2159.
77 C. Shu, R. S. Mega, B. J. Andreassen, A. Noble and V. K. Aggarwal, *Angew. Chem., Int. Ed.*, 2018, **57**, 15430–15434.
78 R. S. Mega, V. K. Duong, A. Noble and V. K. Aggarwal, *Angew. Chem., Int. Ed.*, 2020, **59**, 4375–4379.
79 A. Whyte and T. P. Yoon, *Angew. Chem., Int. Ed.*, 2022, **61**, e202213739.
80 N. A. Till, R. T. Smith and D. W. C. MacMillan, *J. Am. Chem. Soc.*, 2018, **140**, 5701–5705.
81 H. Yue, C. Zhu, R. Kancherla, F. Liu and M. Rueping, *Angew. Chem., Int. Ed.*, 2020, **59**, 5738–5746.
82 M. M. Mastandrea, S. Cañellas, X. Caldentey and M. A. Pericàs, *ACS Catal.*, 2020, **10**, 6402–6408.
83 G. A. Lutovsky, S. N. Gockel, M. W. Bundesmann, S. W. Bagley and T. P. Yoon, *Chem*, 2023, **9**, 1610–1621.
84 S.-C. Kao, K.-J. Bian, X.-W. Chen, Y. Chen, A. A. Martí and J. G. West, *Chem. Catal.*, 2023, **3**, 100603.
85 P. Nilges, T. R. dos Santos, F. Harnischa and U. Schröder, *Energy Environ. Sci.*, 2012, **5**, 5231–5235.
86 I. Cabasso, M. Li and Y. Yuan, *RSC Adv.*, 2012, **2**, 9998–10006.
87 L. Wu, M. Mascal, T. J. Farmer, S. P. Arnaud and M.-A. W. Chang, *ChemSusChem*, 2017, **10**, 166–170.
88 Y. Hioki, M. Costantini, J. Griffin, K. C. Harper, M. P. Merini, B. Niss, Y. Kawamata and P. S. Baran, *Science*, 2023, **380**, 81–87.
89 J.-J. Dai, Y.-B. Huang, C. Fang, Q.-X. Guo and Y. Fu, *ChemSusChem*, 2012, **5**, 617–620.
90 R. Matthessen, L. Claes, J. Fransaer, K. Binnemans and D. E. De Vos, *Eur. J. Org. Chem.*, 2014, 6649–6652.
91 X. Shao, Y. Zheng, L. Tian, I. Martín-Torres, A. M. Echavarren and Y. Wang, *Org. Lett.*, 2019, **21**, 9262–9267.
92 P. Qian, Z. Yan, Z. Zhou, K. Hu, J. Wang, Z. Li, Z. Zha and Z. Wang, *J. Org. Chem.*, 2019, **84**, 3148–3157.
93 A. F. Garrido-Castro, Y. Hioki, Y. Kusumoto, K. Hayashi, J. Griffin, K. C. Harper, Y. Kawamata and P. S. Baran, *Angew. Chem., Int. Ed.*, 2023, **62**, e202309157.
94 M.-X. Shen, C.-Q. Deng, J. Yang and J. Deng, *Green Chem.*, 2024, **26**, 10290–10298.
95 A. Trowbridge, S. M. Walton and M. J. Gaunt, *Chem. Rev.*, 2020, **120**, 2613–2692.

